

Lipid Nanotubes as an Organic Template for an Electrically-Conductive Gold Nanostructure Network

Kristina Jajcevic¹, Kaori Sugihara²

¹Department of Physical Chemistry, University of Geneva, Quai Ernest Ansermet 30, 1211 Geneva 4, Switzerland

²Institute of Industrial Science, The University of Tokyo, 4-6-1 Komaba Meguro-Ku, Tokyo 153-8505, Japan

Table S1. IR-absorption bands and assignments

Assignments		
Wavenumber (cm ⁻¹)	Dried lipids	Fixed lipids
3340		O-H group
3300	N-H group	
2926	C-H asymmetric stretching	C-H asymmetric stretching
2853	C-H symmetric stretching	C-H symmetric stretching
1735		C=O ester or aldehyde
1724	C=O ester (from lipids)	
1695	C=C alkene	
1644		C=C alkene or C=N imine
1639	C=C alkene	
1558	N-H group	
1448	C-H alkane	C-H alkane

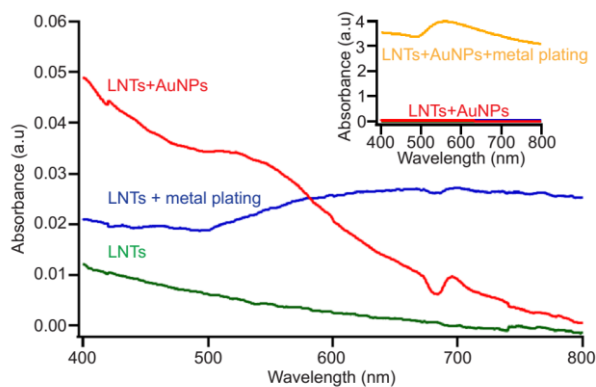


Figure S1: Ultraviolet-visible (UV-VIS) spectra of LNTs (green), after metal plating (blue), after attachment of Au nanoparticles (AuNP) (red), and after attachment of AuNPs and the metal plating (yellow) in the inset.

Control experiments for the metal plating process. To prove that Au nanowires in our system only form in the presence of aligned AuNPs on LNTs, we performed the metal plating on several control samples. UV-VIS spectroscopy was used for the characterization, because both AuNPs and Au nanowires present a characteristic plasmonic peak in absorption spectra.¹⁻³ First, LNTs without AuNPs show no clear absorption peak (green in Figure S1). When the metal plating was performed on these LNTs without AuNPs, the absorption spectra altered, yet no clear peak was observed (blue in Figure S1). On comparison, when AuNPs are attached to the LNTs, an absorption peak was observed at around 520 nm (red in Figure S1), which corresponds to the expected plasmonic peak from AuNPs.¹⁻² A further metal plating of these LNT-AuNP complexes present 100 times higher plasmonic peak from the grown Au nanowires (yellow in the inset of Figure S1). These results show that the metal plating is not successful unless the AuNPs are pre-deposited along the LNTs for catalyzing the reaction.

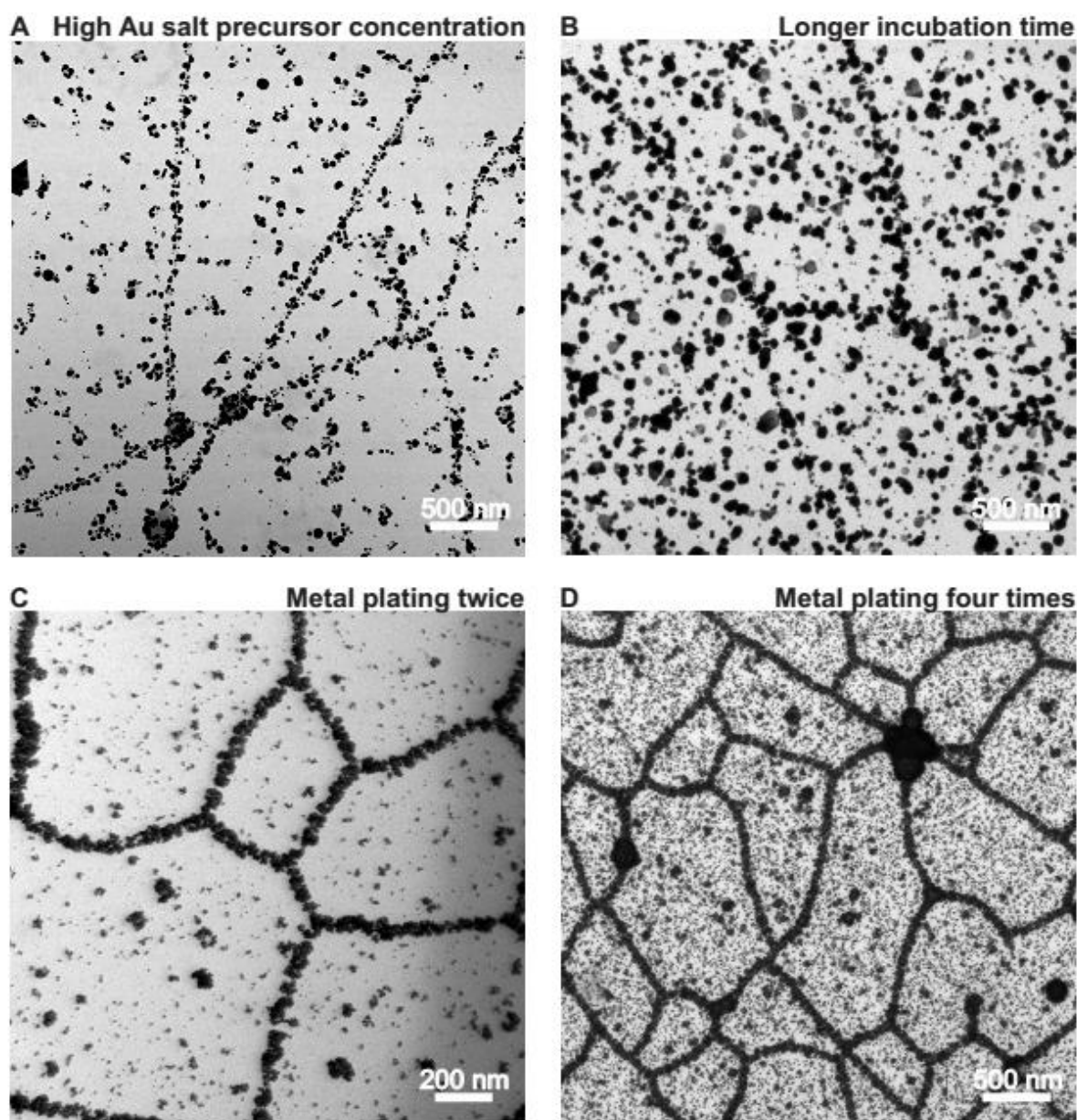


Figure S2: The optimization of the parameters for the metal plating. Transmission electron microscopy images, where the effect of (A) higher Au salt precursor concentration (29.4 mM), (B) longer metal plating incubation time (30 min instead of 5 min), and performing metal plating (C) twice or (D) four times were studied.

Optimization of the metal plating procedure. In the main manuscript we employed a metal plating method based on the previously-reported technique for growing thin gold films on poly(vinyl pyrrolidone) platinum-loaded capsules.⁴⁻⁵ Here, we present our attempt in using another protocol (other reducing agents).⁶⁻⁷ which did not work well even after varying different parameters such as the use of a high Au salt precursor concentration (e.g. 29.4 mM,

Figure S2A), a longer metal plating incubation time (30 min instead of 5 min used in the main manuscript, Figure S2B), and performing metal plating multiple times consecutively at a lower Au salt precursor concentration (0.29 mM, two times, Figure S2C, and four times, Figure S2D, instead of once performed in the main manuscript), because the resulted Au structures were either disconnected (Figure S2B) or a significant background Au adsorption took place (Figure S2CD). We found that these failures were linked to a lack of the fast and efficient metal formation on the substrate and the excess formation of additional AuNPs in solution^{6, 8} that absorbed on the background. These results suggest that the choice of the reducing agent is a critical parameter for optimizing the protocol for our application.

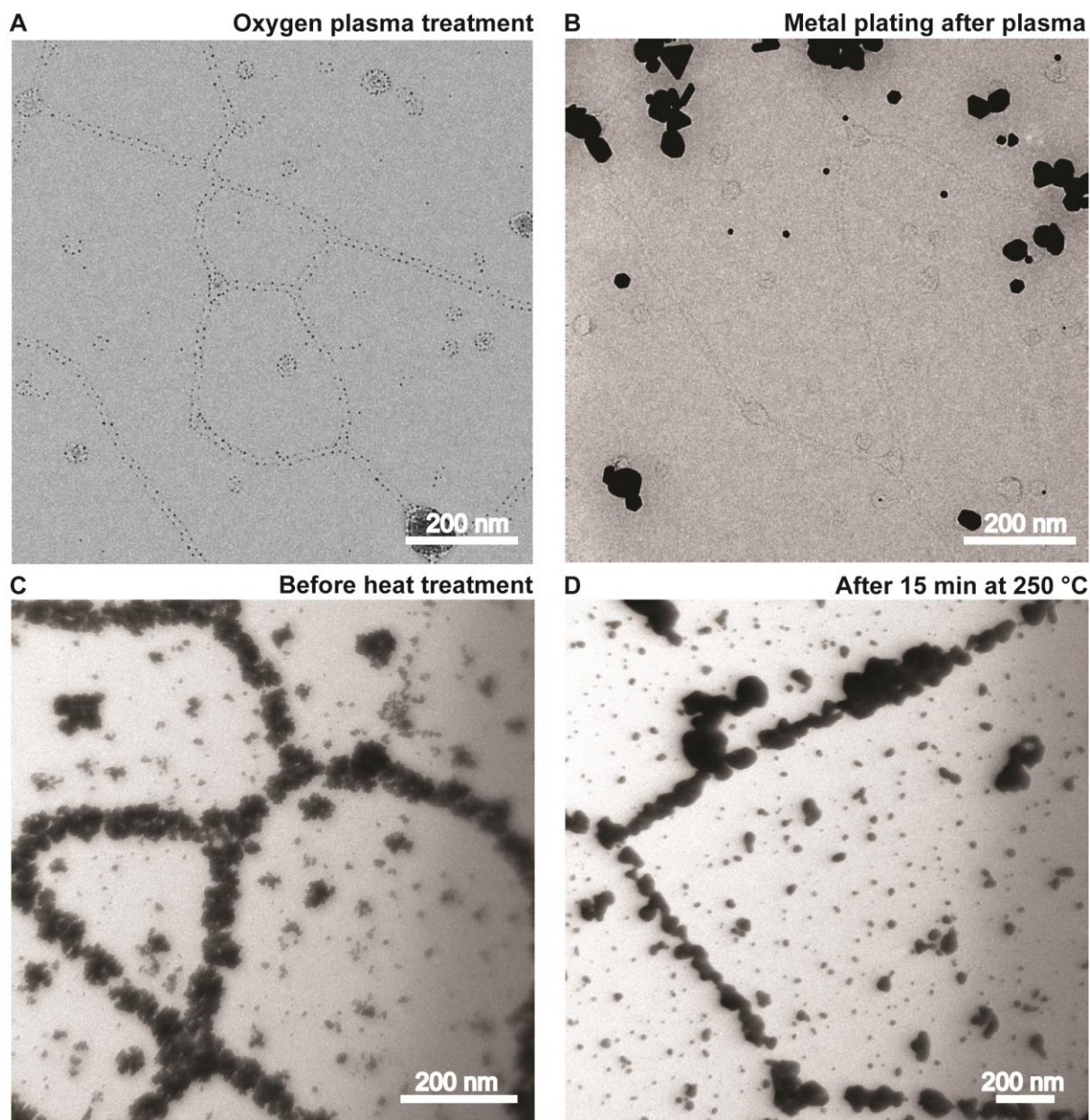


Figure S3: Transmission electron microscopy images, where the effect of (A) the oxygen plasma treatment after the attachment of AuNPs for removing the organic template, (B) the subsequent metal plating, and (C, D) the effect of annealing on the formed Au nanowires were studied.

The effect of the oxygen plasma treatment and the annealing on the samples. The effect of the oxygen-plasma treatment after the attachment of AuNPs (before metal plating) for removing the organic LNT template was studied. The oxygen plasma treatment successfully removed the LNT template without disturbing the alignment of the AuNPs (Figure S3A). However, metallization of these samples failed to connect the AuNPs into wires (Figure S3B),

mainly because these AuNPs without the LNT template easily detached from the substrate during the metal plating. In addition, we also studied the effect of annealing after the Au nanowires were formed. Previously, we have already recognized the difficulty in incorporating the annealing in the Au nanowire fabrication process due to the pearling effect because of the high surface tension of liquid gold.⁹ In general, the temperature at which this pearling effect takes place depends on the feature size of gold. In the present work, the annealing after the metal plating similarly induced the pearling that is difficult to control (Figure S3CD), thus was omitted in the final protocol. This also indicates that the final metal mesh structure has a thermal stability below a few hundred °C.

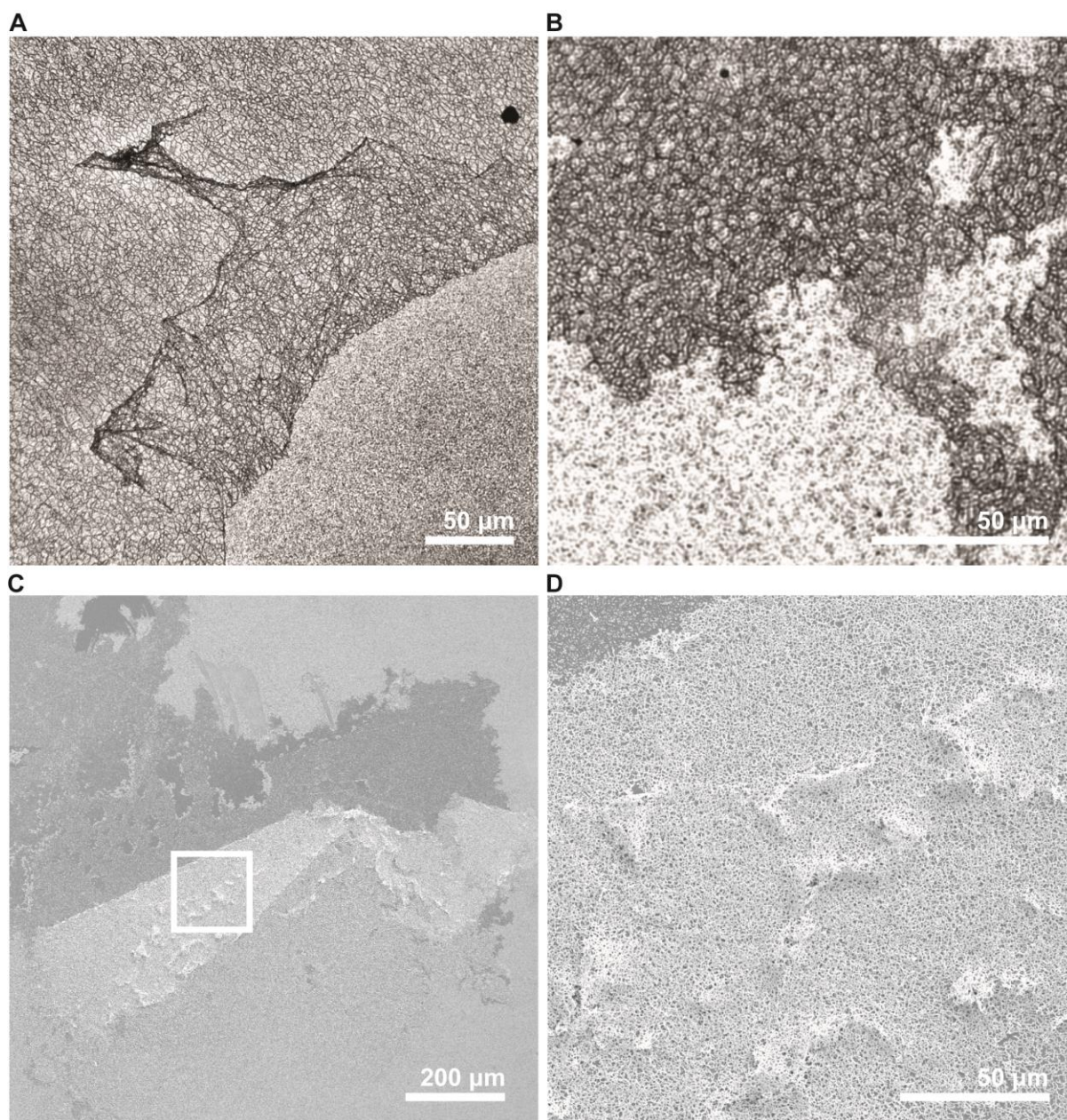


Figure S4: Bright field microscopy images of Au nanowire meshes with areas of (A) folded wires (B) and detached wires. (C) A scanning electron microscopy (SEM) image of a folded Au nanowire mesh on glass surface, where a zoom-in image indicated with a square is shown in (D).

3D structures observed during the sample fabrication process. During the sample fabrication, we occasionally observed detachment and the re-adhesion of the final Au nanowires on the glass substrates. Sometimes, Au nanowires were folded, leaving an area without Au nanowires (Figure S4AC) or wrinkles Figure S4D). If samples are handled too violently, Au nanowires were complete detached (Figure S4B). These disturbance of the metal

mesh strongly affects the conductance, although if it is controlled such a metal mesh 3D structure may find its own application.

Table S2. Material cost per 1 cm² in USD

Material	USD/cm²
Polymer	0.245
Streptavidin	0.002
Lipids	0.937
AuNPs	0.004
HAuCl ₄	4.459
TOTAL	5.647

Estimated average cost for the total sample preparation was calculated. The calculation is based on the concentration used per 1 cm² and given in Table S2. The price can be reduced by 10 times if we replace HAuCl₄ with CuSO₃. To test whether our LNT template approach also works with copper, we attempted different copper metal plating protocols, leaving the rest of the procedure the same as the one described in the manuscript.

Protocol 1

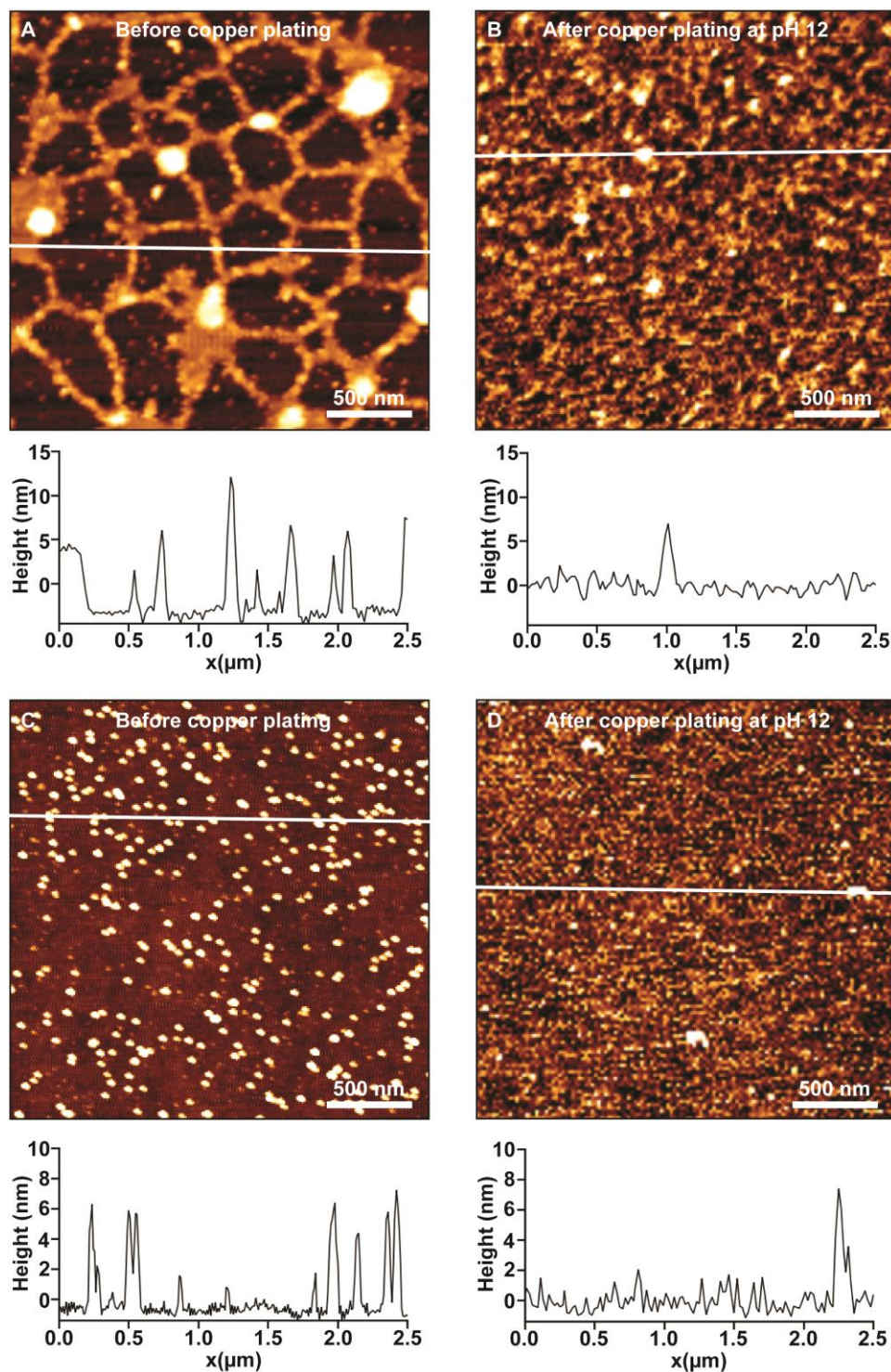


Figure S5: AFM images of AuNP coated LNTs before (A) and after (B) copper plating at basic pH and AuNPs attached to PLLgPEG before (C) and after (D) copper plating under basic pH described in the text as Protocol 1. Corresponding cross sections are all taken at the white lines indicated in each image.

Protocol 1: Copper can be reduced to metal from copper sulphate with formaldehyde under basic conditions at pH around 12. This method has been shown to work in various papers to

grow wires using DNA and rod like viruses as templates with palladium as catalyst for seeding in most cases.¹⁰⁻¹¹ However, this method could not be adopted to our samples as the basic condition deprotonated amine group of PLL, and as a result PLL lost positive charge to hold the wires to the negatively-charged glass substrates (see the above Figure S5). The above Figure S5 A and B in protocol 1 show fixed and dried LNTs with AuNPs before and after copper plating at pH 12. The LNTs are destroyed during the plating process. Figure S5 C and D in protocol 1 show AuNPs directly attached on the PLLgPEG-Biotin before and after copper plating at pH 12. This is a control to show that it is in fact the polymer layer that is detached at pH 12.

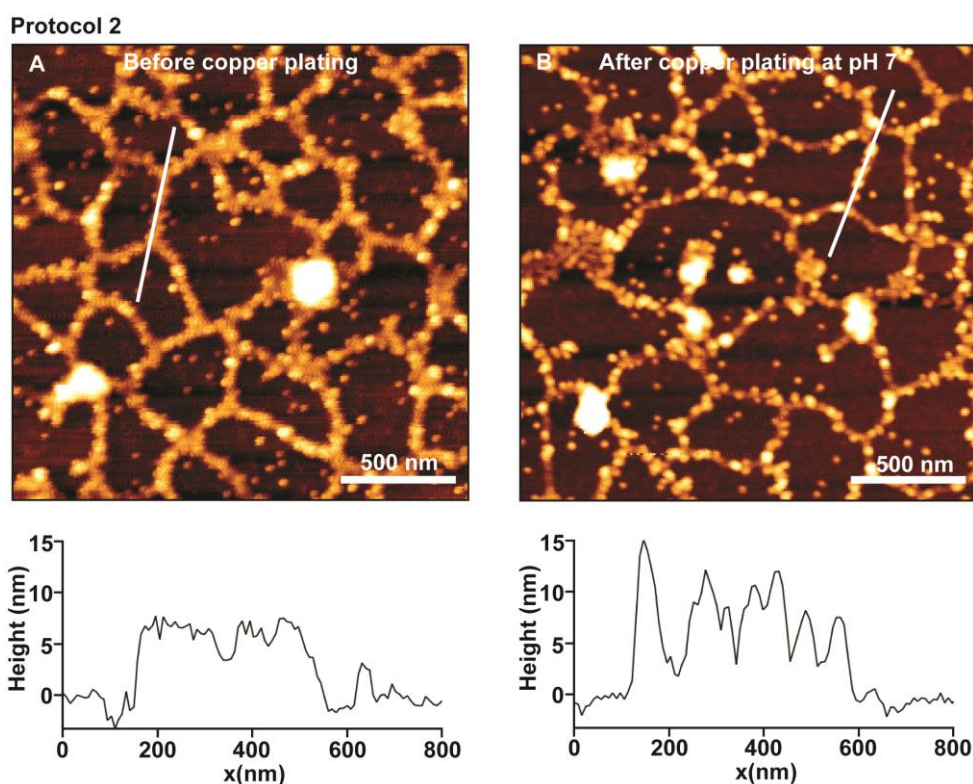


Figure S6: AFM images of AuNP coated LNTs before (A) and after (B) copper plating following Protocol 2. Corresponding cross sections are taken at the white lines indicated in each image.

Protocol 2: We attempted to use sodium borohydride as reducing agent with copper chloride (2:1 ratio) at neutral pH and we have obtained some preliminary results showing slight gold

nanoparticles grew after the metal plating (Protocol 2 in Figure S6 A and B). The protocol was adopted from the ones for the synthesis of copper nanoparticles¹², yet further optimization is required to connect the particles into wires.

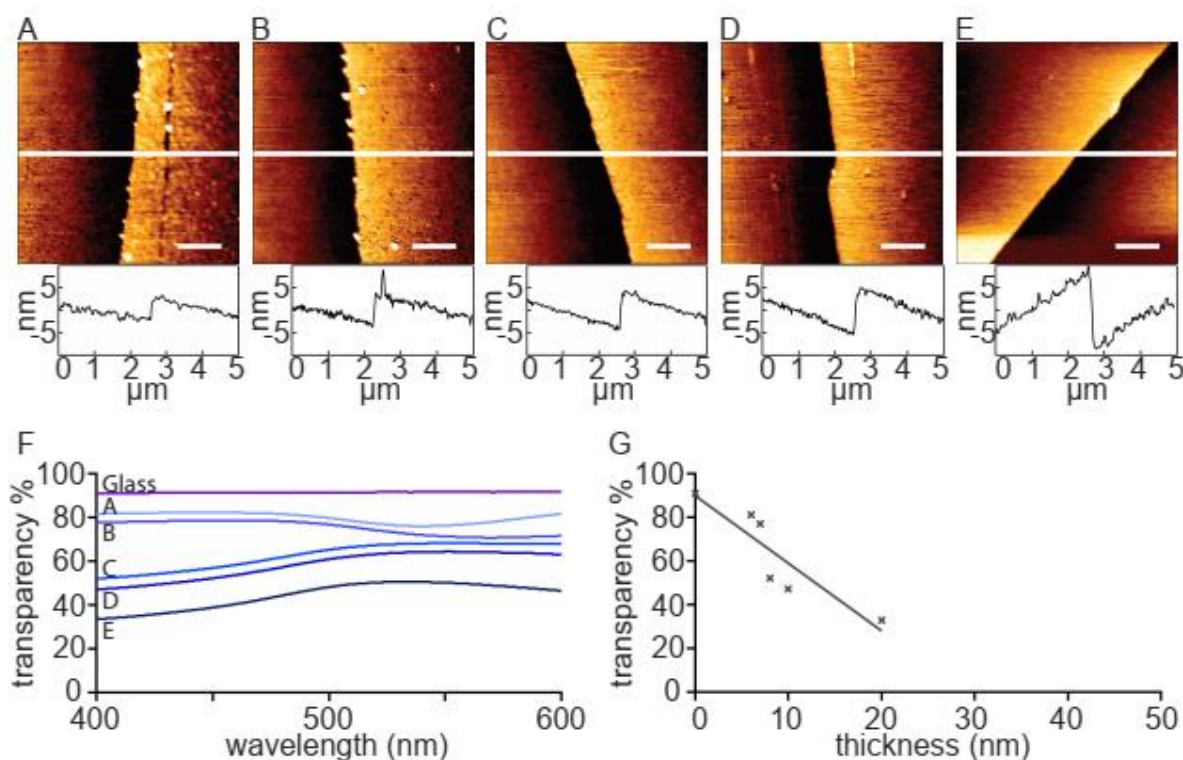


Figure S7: Different thicknesses of sputtered gold on glass surfaces and their corresponding transparency

Correlation between transparency and thickness of gold film sputtered on glass substrates show that there is a decrease in transparency with decreasing film height. Different thicknesses of gold was sputtered on glass substrates and transparency was determined with UV-VIS spectrometry. Heights were determined with AFM by scratching the surface to see the difference between the glass and the gold film.

References

- (1) Chen, M. J.; He, Y. R.; Liu, X.; Zhu, J. Q.; Liu, R., Synthesis and Optical Properties of Size-Controlled Gold Nanoparticles. *Powder Technology* **2017**, *311*, 25-33.
- (2) Bastus, N. G.; Comenge, J.; Puntès, V., Kinetically Controlled Seeded Growth Synthesis of Citrate-Stabilized Gold Nanoparticles of up to 200 Nm: Size Focusing Versus Ostwald Ripening. *Langmuir* **2011**, *27*, 11098-11105.
- (3) Bromley, K. M.; Patil, A. J.; Perriman, A. W.; Stubbs, G.; Mann, S., Preparation of High Quality Nanowires by Tobacco Mosaic Virus Templating of Gold Nanoparticles. *Journal of Materials Chemistry* **2008**, *18*, 4796-4801.
- (4) Hitchcock, J. P.; Tasker, A. L.; Baxter, E. A.; Biggs, S.; Cayre, O. J., Long-Term Retention of Small, Volatile Molecular Species within Metallic Microcapsules. *Acs Applied Materials & Interfaces* **2015**, *7*, 14808-14815.
- (5) Tasker, A. L.; Hitchcock, J.; Baxter, E. A.; Cayre, O. J.; Biggs, S., Understanding the Mechanisms of Gold Shell Growth onto Polymer Microcapsules to Control Shell Thickness. *Chemistry-an Asian Journal* **2017**, *12*, 1641-1648.
- (6) Lin, N.; Zhang, W. X.; Koshel, B. M.; Cheng, J. X.; Yang, C., Spatially Modulated Two-Photon Luminescence from Si-Au Core-Shell Nanowires. *Journal of Physical Chemistry C* **2011**, *115*, 3198-3202.
- (7) Brinson, B. E.; Lassiter, J. B.; Levin, C. S.; Bardhan, R.; Mirin, N.; Halas, N. J., Nanoshells Made Easy: Improving Au Layer Growth on Nanoparticle Surfaces. *Langmuir* **2008**, *24*, 14166-14171.
- (8) Nath, S.; Ghosh, S. K.; Panigrahi, S.; Pal, T., Aldehyde Assisted Wet Chemical Route to Synthesize Gold Nanoparticles. *Indian Journal of Chemistry Section a-Inorganic Bio-Inorganic Physical Theoretical & Analytical Chemistry* **2004**, *43*, 1147-1151.
- (9) Jajcevic, K.; Chami, M.; Sugihara, K., Gold Nanowire Fabrication with Surface-Attached Lipid Nanotube Templates. *Small* **2016**, *12*, 4830-4836.
- (10) Geng, Y. L.; Pearson, A. C.; Gates, E. P.; Uprety, B.; Davis, R. C.; Harb, J. N.; Woolley, A. T., Electrically Conductive Gold- and Copper-Metallized DNA Origami Nanostructures. *Langmuir* **2013**, *29*, 3482-3490.
- (11) Zhou, J. C.; Soto, C. M.; Chen, M. S.; Bruckman, M. A.; Moore, M. H.; Barry, E.; Ratna, B. R.; Pehrsson, P. E.; Spies, B. R.; Confer, T. S., Biotemplating Rod-Like Viruses for the Synthesis of Copper Nanorods and Nanowires. *Journal of Nanobiotechnology* **2012**, *10*, 18.
- (12) Soomro, R. A.; Sherazi, S. T. H.; Sirajuddin; Memon, N.; Shah, M. R.; Kalwar, N. H.; Hallam, K. R.; Shah, A., Synthesis of Air Stable Copper Nanoparticles and Their Use in Catalysis. *Advanced Materials Letters* **2014**, *5*, 191-198.